Implicit Emotion Communication: EEG Classification and Haptic Feedback

RODRIGO CEBALLOS, BEATRICE IONASCU, WANJOO PARK, and MOHAMAD EID,
New York University Abu Dhabi

Today, ubiquitous digital communication systems do not have an intuitive, natural way of communicating emotion, which, in turn, affects the degree to which humans can emotionally connect and interact with one another. To address this problem, a more natural, intuitive, and implicit emotion communication system was designed and created that employs asymmetry-based EEG emotion classification for detecting the emotional state of the sender and haptic feedback (in the form of tactile gestures) for displaying emotions for a receiver. Emotions are modeled in terms of valence (positive/negative emotions) and arousal (intensity of the emotion). Performance analysis shows that the proposed EEG subject-dependent emotion classification model with Free Asymmetry features allows for more flexible feature-generation schemes than other existing algorithms and attains an average accuracy of 92.5% for valence and 96.5% for arousal, outperforming previous-generation schemes in high feature space. As for the haptic feedback, a tactile gesture authoring tool and a haptic jacket were developed to design tactile gestures that can intensify emotional reactions in terms of valence and arousal. Experimental study demonstrated that subject-independent emotion transmission through tactile gestures is effective for the arousal dimension of an emotion but is less effective for valence. Consistency in subject-dependent responses for both valence and arousal suggests that personalized tactile gestures would be more effective.

CCS Concepts: • **Computer systems organization** → **Embedded systems**; *Redundancy*; Robotics; • **Networks** → Network reliability;

Additional Key Words and Phrases: Affective computing, affective haptics, multimodal interaction, tactile gestures

ACM Reference format:
Rodrigo Ceballos, Beatrice Ionascu, Wanjoo Park, and Mohamad Eid . 2017. Implicit Emotion Communication: EEG Classification and Haptic Feedback. *ACM Trans. Multimedia Comput. Commun. Appl.* 14, 1, Article 3 (December 2017), 18 pages.
https://doi.org/10.1145/3152128

1 INTRODUCTION

Advances in communications technology have recently made it possible for people to communicate information with unprecedented ease. In particular, these improvements have begun to provide alternatives to natural channels of communication that are not always available because of either distance, disability, or other issues.

This work is supported by the New York University Abu Dhabi.
Authors' addresses: R. Ceballos, B. Inoascu, W. Park and M. Eid, Applied Interactive Multimedia Research Lab (AIMLab), Lab 5, Experimental Research Building (C1), New York University Abu Dhabi, Saadiyat Island, P.O. Box 129188, United Arab Emirates; emails: {rceballos98, beatrice.nsc}@gmail.com, {wanjoo, mohamad.eid}@nyu.edu.

https://doi.org/10.1145/3152128

These improvements, however, have only concerned themselves with the technical aspects of information communication and have, to some extent, disregarded the way in which this information is acquired and displayed. In particular, the transmission of emotional information has lacked many of the tools that we naturally use to transmit this sort of information, such as implicit signals through tone, pitch, and body language that are both expressed and understood subconsciously [8].

This subconscious element is what is missing from current digital communication systems, which require conscious actions by both the person transmitting the message and the person interpreting it. It is precisely this gap between natural, face-to-face interactions and digital communication technologies that our proposal attempts to bridge through the creation of an implicit emotion communication system.

Building such a system would first require the ability to determine the emotional state of a subject without the individual's conscious input. Human–Computer Interaction (HCI) research has been working on this problem for over a decade now, focusing on easily measured physiological signals such as galvanic skin response, facial electromyography, and heart rate variability (HRV) [2, 37] to effectively measure the intensity, time and duration of a given emotional state. However, in order to measure the valence dimension of emotion, EEG measurements of the prefrontal cortex have been found to be the most accurate [7, 31].

Regarding the display of emotion, given how touch is intrinsically emotional [11], haptic feedback has been shown to be an attractive alternative to conventional methods since it is particularly effective at communicating valence and arousal [13]. This linkage between haptic interactions and emotional states has even been observed in experiments in which subjects were not consciously aware of the haptic feedback or of its intended effect on their emotions [13]. This evidence hints at the idea that haptics could provide a more intrinsic display for emotion that, to some degree, can be subconsciously and intuitively interpreted.

1.1 Implicit Emotion Communication Systems

In spite of the breakthrough of digital communication during the past decades, there has not been a particularly strong incentive to create specialized networks for implicit emotional transmission. Many emotion clues are conveyed verbally; however, emotions are sometimes expressed subliminally, nonverbally, and even unconsciously [29]. Since current methods require people to consciously convey information by typing [34, 38] or by the use of emoticons [16, 18], many of these subliminal messages are not sent.

All work focused on the implicit dimension of emotion so far has been restricted to either emotion recognition or emotion stimulation; however, enough work has been done in these areas recently so that building a proof of concept system that connects the two could be possible.

1.2 EEG-Based Emotion Recognition

Among the approaches to emotion recognition, methods based on electroencephalogram (EEG) signals are more reliable because of higher accuracy and objective evaluation compared to other physiological signals and external appearance methods, such as facial expression and gesture recognition [5, 10, 17]. Recent years have seen a great increase in the analysis of EEG data with machine-learning tools to interpret and classify brain activities, such as recognizing emotional states [17].

Many state-of-the-art implementations of machine-learning algorithms focus heavily on neuroscience-based feature extraction and feature generation methods that, so far, have yielded promising results [17]. Soleymani et al. [32] proposed a user-independent emotion recognition method with EEG and eye gaze data, using logarithms of Power Spectral Density (PSD) as EEG features. Results demonstrated accuracies of 68.5% for three labels of valence and 76.4% for three

labels of arousal using a modality fusion strategy and a support vector machine (SVM). Duan et al. [12] first introduced differential entropy to emotion recognition and then compared discriminative properties of different features. They used SVM as a classifier and achieved an average accuracy of 81.17%. Wang et al. [35] systematically compared three kinds of EEG features (power spectrum feature, wavelet feature, and nonlinear dynamical feature) for emotion classification. They proposed an approach to track the trajectory of emotion changes with manifold learning.

In particular, the PSD of specific frequency bands in the EEG spectrum from different regions of the brain has been combined to create asymmetry features that, to some degree, attempt to represent the change in PSD of these frequency bands across the surface of the scalp [17, 26, 39].

Currently, all research being done on this topic uses similar electrode pairs to generate these asymmetry features, usually being mirror electrodes across the left and right hemispheres of the brain. This means that features are restricted to changes in the PSD on this spatial dimension. While so far these kinds of features have been relatively successful, novel efforts [39] are moving away from just including gradient changes across this dimension and try to include features that pair mirrored electrodes across the frontal-caudal axis.

Since 2-D plots of PSD across the scalp show that asymmetries across the brain vary in several spatial directions, creating features that contain this information might lead to better results during classification.

1.3 Haptic-Based Emotion Display

In the field of communication, the research community has taken special interest in the idea of including emotions in the realm of technology-powered human-to-human communication. Research has shown that one of the most effective ways to accomplish emotional communication is through the use of nonvisual, nonverbal cues, such as touch [14]. It is not surprising, then, that current efforts are being placed in the development of affective haptic systems that integrate technology with the evocation and recognition of emotions. The final goal for these technologies is the accurate and effective transmission of emotions to human users.

To enhance emotional communication in traditional remote teleconferencing, Cha et al. [9] proposed HugMe, a synchronous haptic system that allows a passive user wearing a haptic jacket to feel the touch of an active user during teleconferencing. The HugMe system shows that haptic feedback successfully incorporates emotion elicitation into a traditional communication system. Consistent with this trend, attempts have been made to integrate affective haptics into preexisting systems for digitally mediated human interaction. In particular, some systems have been devised to enhance emotional information accessible to physically impaired individuals [23] and others to enhance virtual reality emotional feedback [27].

Similarly, Arafsha et al. [3] developed a wearable haptic system to improve the multimedia experience of a user. In the design of this system, the authors surveyed consumers to create haptic patterns associated with six emotions: love, joy, surprise, anger, sadness, and fear. They used various affective haptic components such as vibration, warmth, heartbeat stimulation, and shivering to successfully increase the engagement of a user while watching short video clips. The implementation of these technologies has led to a search for more general systems that allow for an increasing range of recognizable emotions [4]. Mazzoni and Bryan-Kinns [22], for example, used a haptic glove to transmit a wide range of emotions, finding correlations between frequency and intensity of vibration and valence and arousal responses.

Haptic jackets seem to be the preferred haptic device of choice for a wide majority of the affective haptics research community [3, 9, 20, 27]. Lemmens et al. [20] developed a haptic jacket that renders tactile emotion effects onto the user's body using 64 evenly distributed vibrotactile motors. The authors implemented 40 different tactile patterns based on typical behaviors from

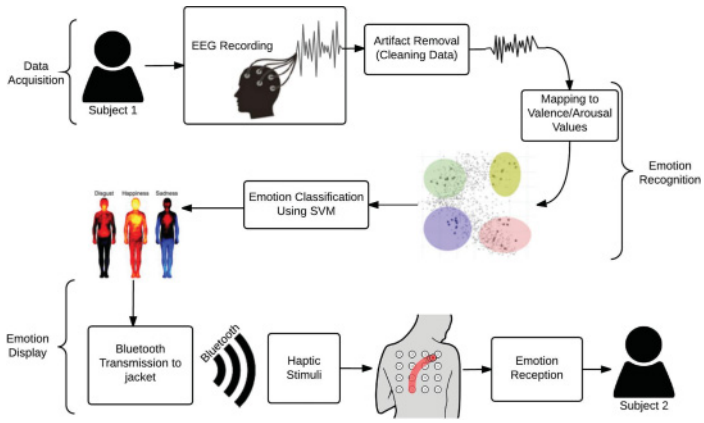

Fig. 1. Proposed framework for an emotion communication system.

human emotional touch interaction, common sayings, or abstract patterns related to a movie clip and found that the addition of these tactile sensations enriches the movie-watching experience. Nummenmaa et al. [25] showed that different emotional feelings are consistently related to statistically distinguishable body sensations, especially pertaining to the torso, neck, and arms [28]. Haptic jackets are thus an effective way of stimulating, eliciting, and influencing the emotional state of a human because they create a haptic sensation on the user's upper body. The complexity of the sensations can range from simple one-point gestures to apparent continuous motion between two vibrating points obtained by varying the frequency, intensity, and duration of stimulation [15].

2 PROPOSED FRAMEWORK

A comprehensive framework is designed to capture affective features without user input, map these features to haptic gestures, and display the generated haptic gestures using the haptic jacket [21]. Three main steps compose this framework, as depicted in Figure 1.

2.1 Data Acquisition

An implicit way to extract emotional reactions is by examining brain discharge. Therefore, the first step calls for extracting affective features from a user without the individual's conscious input via EEG and mapping these features into a continuous-valued scale of arousal (how intense the emotion is) and valence (how positive or negative the emotion is).

Without loss of generality, each dimension in this space can be normalized to take values in the range of [-1,+1]. Estimating emotions on a continuous-valued scale provides an essential framework for recognizing dynamics in emotions, tracking intensities in the course of time, and adapting to individual moods or personalities.

Research has been conducted to extract features that are correlated with arousal and/or valence [33]. For instance, informative features for arousal estimation include loudness and energy of the audio signal, motion component, visual excitement, and shot duration. Features that correlate to valence include lighting, saturation, color energy, rhythm regularity, and pitch.

In this study, EEG signals were utilized to train user-specific classifiers that could accurately map raw EEG data into the valence-arousal space without any conscious subject input.

Fig. 2. Haptic jacket design.

2.2 Emotion Recognition

The second step comprises mapping the identified emotional responses (valence arousal) into a corresponding tactile gesture that can be displayed using the haptic jacket. The concept is to generate a haptic cue that is capable of highlighting specific emotional reactions. For instance, when high arousal is identified, abrupt and high-intensity vibration is generated. In general, a tactile gesture is characterized by the intensity, frequency, direction of vibration, the mode of tactile motion (discrete vs. continuous), and the position of tactile stimulation. Therefore, a valence-arousal state would be mapped to continuous values representing these attributes that eventually shape the perception of the tactile gesture.

Affective haptics research shows that the valence dimension of emotion is closely related to the frequency, continuity, position, and direction of perceived movement [15, 30, 37]. Based on these findings, a mapping of the valence dimension of emotion to tactile gesture based on these parameters is implemented. A subsequent study suggested that a position-based mapping for valence is not the most effective to intensify emotional reactions [25, 28]. The study concluded that the perceived direction of tactile gesture is more effective. Therefore, valence is mapped through frequency, intensity, and direction (position was less effective). On the other hand, the arousal dimension of emotion is closely related to the intensity and frequency of the tactile stimulation [22]. Therefore, a mapping of the arousal dimension of emotion is implemented based on intensity, frequency, and direction.

2.3 Emotion Display

A tactile gesture is an apparent motion of tactile stimulation that can convey a particular message to the recipient. These gestures are rendered using a custom-made haptic jacket that was build at the Applied Interactive Multimedia lab of New York University Abu Dhabi. The jacket is a garment with embedded actuators (a total of 48) that can render tactile stimuli (Figure 2). Tactile stimulation can be applied anywhere on the upper body (arms, shoulders, back and abdomen areas). A zipper allows for easy access to the actuators. The jacket, with all the hardware elements mounted, weighs 750 grams.

The hardware design comprises 48 actuators distributed on the jacket, flexible cabling, and a Printed Circuit Board (PCB) that hosts the actuator control circuitry. A microcontroller (Arduino Nano microcontroller), three 16-channel TLC drivers, a Bluetooth module, and a step-up regulator constitute the control circuitry. The microcontroller is programmed to receive serial commands from an external application (via Bluetooth) to activate the actuators. The 16-channel TLC drivers

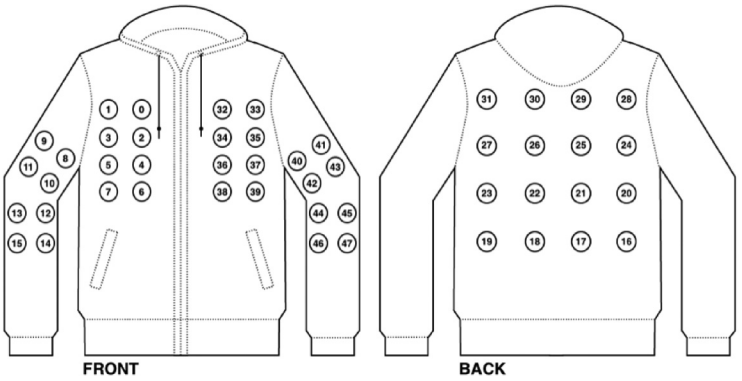

Fig. 3. Schematic showing the distribution of actuators on the front, arms, and back of the jacket.

are Pulse Width Modulation (PWM) units with 12-bit duty cycle control (0–4,095). The PWM technique is used to control the effective power supplied to the actuators and eventually the intensity of vibration. The three TLC drivers are daisy chained to expand the number of PWM outputs to 48 so that the microcontroller can control the 48 actuators simultaneously.

The Bluetooth module (JY-MCU) is used for wireless communication between the microcontroller and the remote application. The PCB circuit is connected to the distributed actuators using flexible cabling. Piezoceramic disk actuators were chosen because they are lightweight, thin, inexpensive, and capable of generating strong, albeit nonaudible, vibration. The distribution of the actuators over the upper body is shown in Figure 3.

3 EEG-BASED EMOTION RECOGNITION

3.1 Acquisition and Preprocessing

Twenty (20) voluntary users (10 male, 10 female), ages between 18 and 35, participated in a paid experiment to test the proposed system. The subjects were right-handed and reported no diagnosed mental or emotional disorders.

A 32-channel Ag/Cl active electrode EEG (BrainAmp DC by BrainProducts[1]) was used to record brain activity. The Brain Vision recording software was used to monitor the EEG data collection and was integrated with Presentation, the stimuli presentation software [24].

The EEG experiment setup is shown in Figure 4. Participants were shown a series of 300 images selected from the IAPS affective picture database [19]. A total of 75 images were chosen from each quadrant of the valence/arousal space, corresponding to the following four groups: Low Valence Low Arousal (LVLA), Low Valence High Arousal (LVHA), High Valence Low Arousal (HVLA), and High Valence High Arousal (HVHA). The images selected for each group were those with the largest Euclidean distance between their reported scores and the margins of other selected groups in order to create four clearly separable groups of images, as shown in Figure 5.

Data acquisition was conducted in university laboratories, in acoustically isolated rooms. Participants were informed about the procedure of the experiment and were asked to sign a consent form. Prior to the experiment, participants were fitted with the 32-channel Ag/Cl active electrode EEG system. Three configurations of the system are considered with 8, 16, and 32 electrodes (as shown in Figure 6). The exact locations of these electrode configurations may slightly change

[1] http://www.brainproducts.com/.

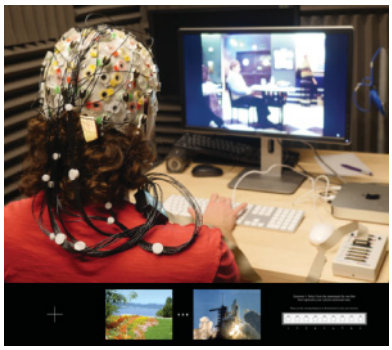

Fig. 4. EEG experiment setup.

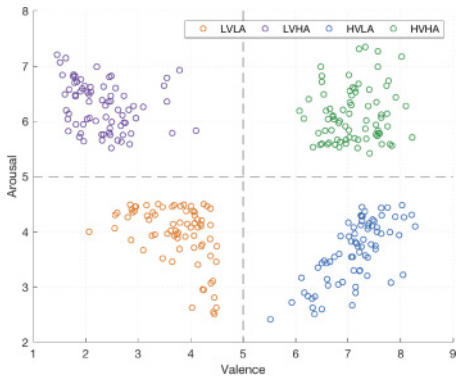

Fig. 5. Selected IAPS picture distribution and grouping displayed on valence/arousal space.

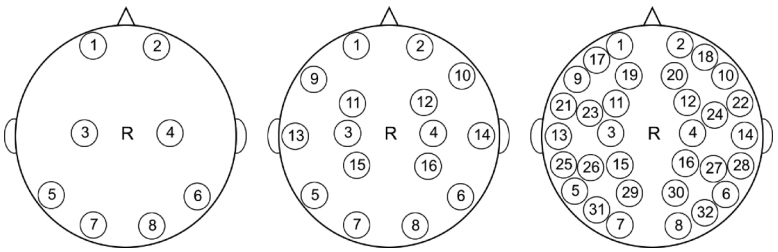

Fig. 6. Schematic showing the locations in 8-, 16-, and 32-electrode configurations.

from one user to another. The configurations of 8 and 16 electrodes are considered due to high availability of commercial EEG devices with these numbers of electrodes.

The experiment was divided into 60 trials, each consisting of a 5-second blank screen, a 5-second countdown, a 1-second cross to focus attention to the middle of the screen, and a succession of 5 images, each shown for 6 seconds. Images shown within the same trial all belonged to the same Valence/Arousal quadrant and were randomly chosen to be a representative sample of the other picture in their group. The order of the trials was random with respect to the Valence dimension and was ordered from low to high with respect to the Arousal dimension to prevent the stronger emotion caused by high arousal images to influence the perception of subsequent low-arousal images [26]. After each trial, participants were asked to rate their emotional response as a function of valence (1-9) and arousal (1-9), using the Self Assessment Manequin (SAM) [6].

3.2 Feature Extraction/Generation

The recorded EEG data was downsampled to 256Hz and passed through a 50Hz notch filter and a 0.5-70Hz band-pass filter to remove signal artifacts. Then, the data was epoched into 60 trials, each consisting of 30-second continuous data of the user viewing 5 pictures from the same affective quadrant. A 5-second sample with a blank screen was used as a baseline for each of the epochs. The EEG features were extracted from the 30-second time windows, as they contained the response to stimuli of the same category.

The PSD for every channel was calculated for all frequency bands shown in Table 1 for each of the 60 trials and used as a feature classification. The logarithm of the PSD was computed and considered as a separate feature, referred to as Differential Entropy (DE).

Table 1. Frequency Bands

Delta (Δ)	$1-3$Hz
Theta (θ)	$4-7$Hz
Alpha (α)	$8-13$Hz
Beta (β)	$14-30$Hz
Gamma (γ)	$31-70$Hz

Free Asymmetry (FA) features were then generated by finding the differences between all DE values across the 5 defined frequency bands and across all possible electrode pairs. Using 32 electrodes, the number of unique electrode pairs was $Fea_N = (32-1)32/2 = 496$; since this process was done across all 5 frequency bands, the total number of features was $Fea_N * 5 = 2480$.

As a baseline comparison to FA, the highest accuracy features DCAU and DASM from [39] were concatenated to create Asymmetry (ASM) features. These features were also computed from DE values and subjected to the same feature selection, classification, and parameter optimization as FA features. The main difference between ASM and FA features is that ASMs are only computed across electrode pairs from different hemispheres (left, right, frontal, and posterior), whereas FA features can be computed from any two electrode pairs irrespective of location.

Finally, in order to both facilitate feature selection and increase classification accuracy, features were normalized and discretized as described by Equation (1). In this equation, α is equal to a normalization resolution parameter that dictates how many standard deviations a given feature must be away from its mean to register a change once discretized.

$$norm(X) = \left\lfloor \alpha \frac{X - \bar{X}}{\sigma_x} \right\rfloor \tag{1}$$

3.3 Feature Selection

A mutual information (Equation (2))–based algorithm (mRMR, Equation (3)) [1] was used to score all generated normalized features, maximizing their mutual information with their respective class and minimizing the mutual information between highly ranked features. From this scoring, the top N asymmetry features were selected to be used by the classification algorithm.

$$I(X;Y) = \sum_{y \in Y} \sum_{x \in X} p(x,y) \log \left(\frac{p(x,y)}{p(x)\,p(y)} \right) \tag{2}$$

$$mRMR = \max_{s} \left[\frac{1}{|s|} \sum_{f_i \epsilon S} I(f_i, c) - \frac{1}{|s|^2} \sum_{f_i, f_j \epsilon S} I(f_i, f_j) \right] \tag{3}$$

3.4 Classification and Optimization

The best N asymmetry normalized features were then used by a linear kernel SVM to classify each trial into one of the four quadrants of the valence/arousal emotional mapping. The accuracy for each trained SVM was calculated using 5 cross-validations.

A grid search optimization algorithm was used to find the optimal normalization resolution factor (α) for a given number of features. During this optimization, the range for α was from 0.1 to 100 and the range for the number of features was from 1 to 600. This space was not explored uniformly but rather an initial sparse search was done to identify regions with higher accuracies.

While each algorithm exhibited different behavior under our optimization routine and arousal classification usually performed better with higher number of features when compared to valence,

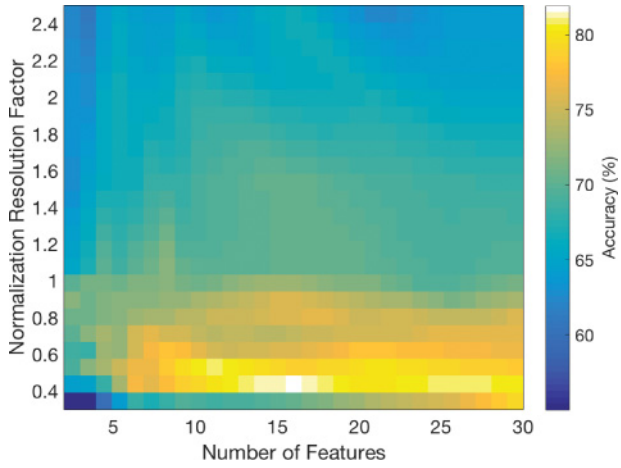

Fig. 7. Grid search optimization of normalization resolution factor and feature number interval [1-30] for valence classification using Free Asymmetry features.

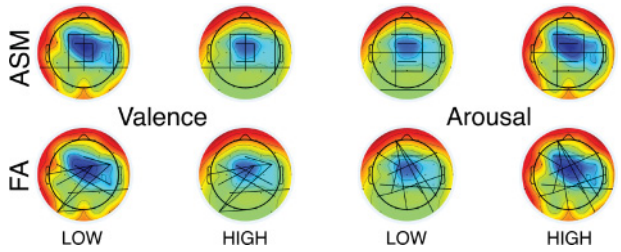

Fig. 8. Sample DE values for the alpha frequency band overlaid with selected features for Asymmetry (ASM) (up) and Free Asymmetry (FA) (down) feature extraction algorithms.

the overwhelming result of the optimization procedure showed that normalization factors between 0.3 and 0.6 were the most effective. Figure 7 shows examples of this optimization process for valence classification.

3.5 Performance Evaluation and Results

3.5.1 Free Asymmetry Features. Figure 8 includes eight 2-D mappings of DE values corresponding to the alpha frequency band across two sample epochs recorded during this study. The plots have been overlaid with lines that show the electrode pairs corresponding to the best 30 selected ASM and FA features.

Figure 8 serves as an example for a qualitative comparison between FA and ASM features. In particular, this example is meant to highlight the general observation that FA features often formed clustering where one or two electrodes have a considerably larger number of features associated with them than the rest, whereas top ASM features were usually more evenly distributed among electrodes.

3.5.2 Classification Accuracy. As mentioned in Section 3.4, all classification accuracies were computed using fivefold cross-validation. Figures 9 and 10 show the maximum average accuracies obtained over all subjects within the shown intervals for a number of features. Each of these results is also optimized in terms of the normalization factor used, such that the reported maximum

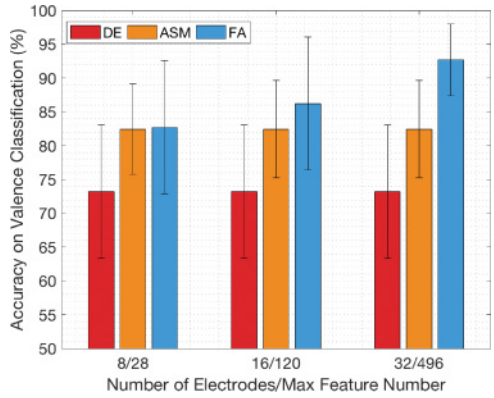

Fig. 9. Maximum classification accuracy for valence on specific feature number intervals for Differential Entropy (DE), Asymmetry (ASM), and Free Asymmetry (FA). Intervals: 1-28 (8 electrodes), 29-120 (16 electrodes), 121-496 (32 electrodes).

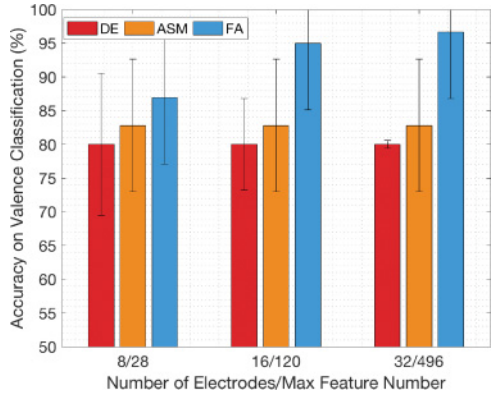

Fig. 10. Maximum classification accuracy for arousal on specific feature number intervals for Differential Entropy (DE), Asymmetry (ASM), and Free Asymmetry (FA). Intervals: 1-28 (8 electrodes), 29-120 (16 electrodes), 121-496 (32 electrodes).

Table 2. FA Accuracies for Select Feature Intervals

Number of Electrodes	Maximum Features	Valence accuracy	Arousal accuracy
8	28	82.5%	87.5%
16	120	86.0%	95.0%
32	496	92.5%	96.5%

accuracies truly represent the best performance that each feature extraction method was able to attain independent of classification parameters.

Table 2 shows the maximum accuracies for valence and arousal classification using free asymmetry features when restricting the number of features to 28, 120, and 496. These intervals were chosen to see how this algorithm would perform under the constraints of EEG devices with fewer

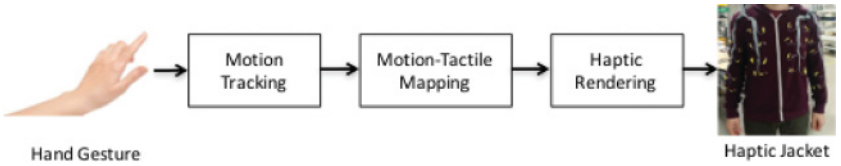

Fig. 11. Tactile gesture authoring tool.

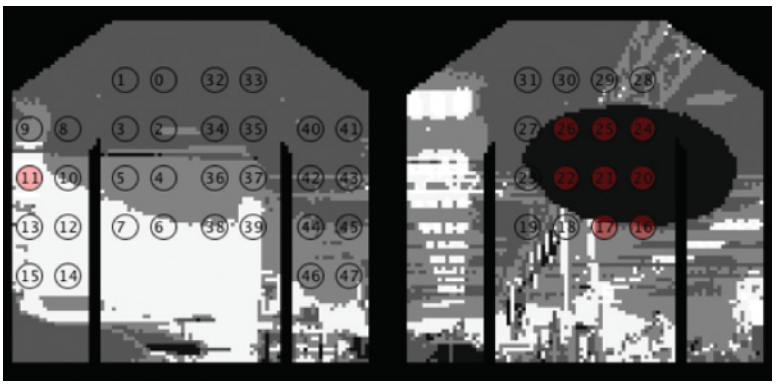

Fig. 12. Tactile gesture authoring tool display showing a live camera feed with an overlaid 2D representation of the haptic jacket and its actuators (numbered circles). Here, the program is looking for "dark" pixels, enough of which will activate (red overlay) a particular actuator. The dark disk shown on the right side of the screen is therefore inducing some activation in the corresponding "back" region of the jacket.

numbers of electrodes, which, in turn, limits the total number of electrode pairs that can be formed to compute asymmetry features.

4 HAPTIC-BASED EMOTION DISPLAY

4.1 Tactile Gesture Authoring Tool

A tactile gesture authoring system is designed to convert a hand gesture into a haptic gesture and then render it via a haptic jacket. As shown in Figure 11, four components comprise this system: Motion Tracking, Motion-Tactile Mapping, Haptic Rendering, and the Haptic Jacket. The Motion Tracker uses a web camera and signal processing to detect the hand and track its movements. The features of hand gestures are translated into tactile gesture features via the Motion-Tactile Mapping component. The Haptic Rendering component displays the tactile gesture via the Haptic Jacket.

The actuators on the jacket are controlled remotely using a custom-made software interface application. The application allows for complete control over each of the 48 actuators by means of a video input interface. This visual interface was chosen in order to provide an intuitive means of generating tactile gestures that can be rendered on the fly. The motion tracking component processes each video frame and identifies the location, size, and distance-to-camera of the hand. The distance-to-camera of the hand is used to define vibration intensity.

Using the video input interface as shown in Figure 12, gestures are created by mapping pixel intensity above a certain threshold into proportional actuation of a specific motor. Specifically, an outline of the front and back views of the jacket, with the positions of the actuators, is shown on a white background and the user is able to manually draw or programmatically overlay a pattern

onto the outline of the jacket, actuating the motors that are closest to the region selected by the user.

After selecting a transmission frequency [5-20Hz], each frame is mapped into a 96-bit matrix that controls the intensity at which each motor is actuated. The indices of the elements refer to the number of the motor, whereas each consecutive two bits refer to the intensity of the vibration in a range of four steps. The motors are numbered 0 to 47, as shown in Figure 12.

The matrix is encoded into a 12-byte packet that is sent over to the microcontroller. The microcontroller is programmed to receive instructions in the form of bytes over a serial port. One byte at a time is read, decoded, and then saved into a matrix in the microcontroller's memory. After 12 bytes are received, the decoded matrix is used to set the output value for each channel. The PWM values are set as follows: 00 corresponds to zero duty cycle or off; 01 corresponds to a quarter of the maximum duty cycle (1023); 10 corresponds to half the maximum duty cycle (2047); and 11 corresponds to three quarters of the maximum duty cycle (3071). The motors are updated at a rate of 20Hz in order to create different vibration patterns and the illusion of apparent motion.

4.2 Tactile Gesture Authoring

A pilot study is conducted with 3 participants to determine the best parameters to convey valence and arousal in an intuitive, self-explanatory way. Both the average recognition rates and debriefing comments provided by the participants are then used to optimize the gestures used in the next iteration of the optimization process. This process is repeated 3 times such that a total of 6 different gestures are tested for each parameter being evaluated (valence and arousal). Given that some subjects report that the back of the jacket is loose, the study is continued without using the back side of the jacket in the haptic stimulus design. One final test round involving the top 5 gestures for each parameter is conducted with a different set of 3 participants to rank the gestures. The results from these pilot tests, shown in Table 3 (valence) and Table 4 (arousal), are used to find the optimal stimulation frequency and intensity of the perceived movement to map both valence and arousal more effectively.

Consequently, four candidate tactile gestures are considered for intensifying valence-arousal reactions (Table 5 lists the configurations for these tactile gestures). As literature describes both arousal and valence as being functions of frequency, we established a linear relationship such that stimulation frequency increases with both arousal and valence.

4.3 Tactile Gesture Optimization

Twenty users participated in the experiment to test the effectiveness of the selected tactile gestures to intensify valence/arousal reactions. Prior to the experiment, participants were fitted with the haptic jacket. During the experiment, participants could press a button to initiate a haptic gesture from the four gestures described in Table 5. Each gesture played on the jacket for 10 seconds. A SAM scale for valence and arousal was given to the user (shown in Figure 13). This procedure was repeated 40 times such that each gesture was rated 10 times using a pseudo-random order to make sure that the same gesture was not repeated twice in a row. During the experiment, participants were not aware of how many total gestures they would test or the parameters used to create them (direction, frequency, and intensity).

4.4 Tactile Gesture Evaluation

Creating an intuitive set of gestures that accurately maps valence irrespective of subject variability proved difficult. While our preliminary tests suggested that direction and frequency could be used effectively to accomplish this goal, a larger sample size showed that valence mapping of haptic gestures is very subject dependent. In this sense, the candidate tactile gestures were not highly

Table 3. Valence Gesture Optimization

Rank	Low Valence	High Valence
1	Frequency: 0.5Hz Mode: Discontinuous Direction: Downwards and Out Position: Front Side and Arms	Frequency: 1.4Hz Mode: Continuous Direction: Upward and In Position: Front Side and Arms
2	Frequency: 0.3Hz Mode: Discontinuous Direction: Out Position: Front Side and Arms	Frequency: 2Hz Mode: Continuous Direction: Upward Position: Front Side and Arms
3	Frequency: 1Hz Mode: Discontinuous Direction: Out Position: Front Side and Arms	Frequency: 1Hz Mode: Continuous Direction: Out Position: Front Side and Arms
4	Frequency: 1Hz Mode: Discontinuous Direction: Downwards Position: Front Side and Arms	Frequency: 2Hz Mode: Continuous Direction: Out Position: Front Side and Arms
5	Frequency: 2Hz Mode: Discontinuous Direction: Upwards and In Position: Front Side and Arms	Frequency: 1Hz Mode: Continuous Direction: Downwards and Out Position: Front Side and Arms

Table 4. Arousal Gesture Optimization

Rank	Low Arousal	High Arousal
1	Frequency: 0.5Hz Intensity: 40%	Frequency: 1.4Hz Intensity: 90%
2	Frequency: 0.7Hz Intensity: 40%	Frequency: 2Hz Intensity: 90%
3	Frequency: 0.5Hz Intensity: 30%	Frequency: 0.5Hz Intensity: 90%
4	Frequency: 0.45Hz Intensity: 50%	Frequency: 2Hz Intensity: 40%
5	Frequency: 1Hz Intensity: 50%	Frequency: 2Hz Intensity: 60%

successful in valence mapping, as shown in Figure 14. On the other hand, arousal was successfully mapped intuitively, as is evident by the fact than in more than 80% of trials, participants correctly associated this metric with the intensity and frequency parameters chosen from our preliminary testing (Figure 14).

Another reason for the particularly low accuracy in valence mapping comes from the fact that users have conflicting but personally consistent mappings between haptic gestures and valence. That is, while users did not agree with each other about the correct mapping between haptic gestures and valence, individual users were still very consistent in their gesture mappings without knowing or being asked to try to rate similar gestures. Figure 15 shows how consistently individual

Table 5. Final Haptic Gesture Mapping Design

	Low Valence	High Valence
High Arousal	Frequency: 0.45Hz Intensity: 50% Mode: Discontinuous Direction: Out Position: Front Side and Arms	Frequency: 1Hz Intensity: 50% Mode: Continuous Direction: Upward Position: Front Side and Arms
High Arousal	Frequency: 0.5Hz Intensity: 90% Mode: Discontinuous Direction: Downwards and Out Position: Front Side and Arms	Frequency: 1.4Hz Intensity: 90% Mode: Continuous Direction: Upward and In Position: Front Side and Arms

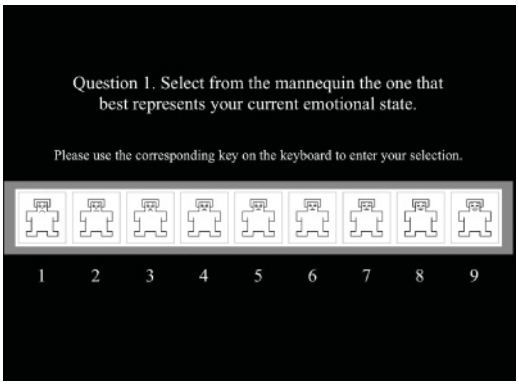

Fig. 13. Sample SAM screen used in EEG and haptic jacket experiments.

subjects rated each gesture: that is, what percentage of their responses for gesture N matched the mode of their responses for that gesture.

To assess the relationship between the authored tactile gestures and the recognition rates for valence and arousal, we performed ANOVA analysis. Significant differences in valence responses were found for the four tactile gestures ($F(2, 636)=3.15$, $p<0.05$). As a result of pairwise comparisons, there is a significant difference in valence between LVLA and HVHL tactile gestures (post-hoc, Tukey-Kraamer). In the case of arousal responses, significant differences were also found for the four tactile gestures ($F(2, 636)=166.31$, $p<0.01$). In results of pairwise comparisons, there are significant difference in arousal between pairs of LVLA/HVHA, LVLA/HVLA, HVLA/LVHA, HVLA/HVHA, and LVHA/HVHA (post-hoc, Tukey-Kraamer). The type of tactile gesture whose sample mean is significantly different from the others can be statistically distinguished and decoded by observing the accuracy rate of the corresponding gesture (Figure 14). The recognition rate for high valence – high arousal emotion is much higher than the false detection rate (an average of 79% recognition rate and less than 10% false detection rate for other tactile gestures). High valence – high arousal tactile gesture contains the mean value of valence/arousal significantly higher than that of the other tactile gestures. Therefore, this tactile gesture is highly correlated to high arousal – high valence. Similarly, high arousal – low valence tactile gesture is highly correlated to high arousal – low valence. A similar ANOVA analysis is conducted to demonstrate the

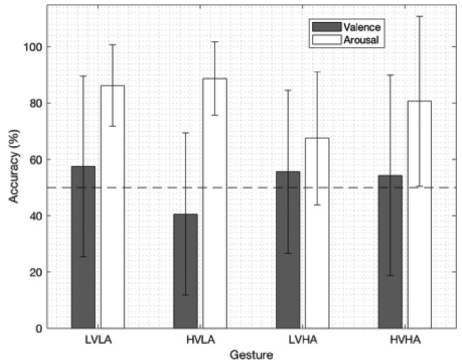

Fig. 14. Average accuracy and standard deviation for valence and arousal mapping of tactile gestures.

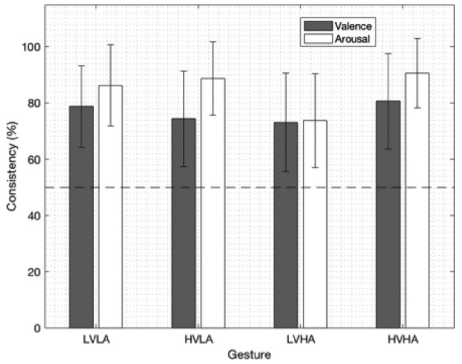

Fig. 15. Average consistency and standard deviation for valence and arousal mapping of tactile gestures.

correlation between low valence – low arousal and the corresponding tactile gesture and between high valence – low arousal and its corresponding tactile gesture.

5 DISCUSSION

Section 3.5.2 shows that while FA features do not perform much better than ASM features when limited to 30 or less features; when allowed to use a higher number of features, this model can attain much higher accuracies for both valence and arousal classification. In particular, as Figure 10 shows, arousal classification can benefit from using FA as a feature extraction method, as it outperforms ASM features by more than 10% in terms of classification accuracy.

As is the case with most EEG-based machine-learning classification studies, the small number of data points and high dimensionality of features always poses the risk of over-fitting. In this study, we have addressed this concern by using cross-validation for all reported accuracies and by using a low normalization resolution factor to make our feature vectors sparse and reduce noise. We have also used a linear kernel SVM as our classification algorithm particularly because of its resilience to overfitting even with low sample sizes.

In terms of the larger context of this study, these results are promising for the future of low-cost, realistic EEG-based emotion recognition systems. The fact that both ASM features and FA features performed with accuracies above 80% with 28 features shows that even EEG devices with 8 electrodes can attain decent classification accuracies, particularly if those electrodes are not fixed to a specific location. Future work in this area is needed to investigate how optimization algorithms could be used to find optimal electrode placements that can be used to maximize subject-dependent EEG emotion classification accuracy.

The results presented in Figure 14 seem to suggest that universal valence gestures might not be possible to achieve with the technology used in this study. Nevertheless, the high accuracy obtained from arousal gestures opens up new possibilities for future haptic systems to validate.

Furthermore, our results regarding subject consistency for both arousal and valence gestures (Figure 15) could lead to advances in subject-dependent gesture generation schemes, which use similar machine-learning techniques to our emotion classifier, to make a personalized intuitive emotion display system. This kind of dynamic gesture-generation system would also make the leap between discrete emotion display to a more fluid transmission within the emotional spectrum defined by valence and arousal. Such a system would be better equipped to pair with our

emotion classifier, which can easily be modified into a regression algorithm that would also produce emotion detection on a spectrum.

Finally, it is important to consider the ethical implications of creating a system capable of accurately detecting and transmitting human emotions. Such a device could have unintended and potentially problematic uses both in interpersonal relationships and as tools for coercion, interrogation, and surveillance. While the system outlined here is probably not practical enough for such ends, future research needs to address the same issues regarding privacy of thought and coercion that all BCI systems need to grapple with.

6 CONCLUSION

This study successfully implemented and verified the performance of ASM features described by [39] on a completely new dataset that used images instead of videos as the emotion elicitation stimuli. In addition, it proposed a new, more complex set of features based on ASM, which vastly outperformed ASM features in high feature space.

It also tested a novel tactile gesture authoring system and haptic jacket design that allowed for intuitive and fast tactile gesture generation and evaluation. These advances might also lead to significant results in the search for universally recognizable arousal haptic gestures and also progress in understanding how to produce equally effective gestures for valence display.

When put together, these two systems make the basis for an intuitive, subconscious emotion communication system that can transmit emotions over a digital network.

7 ACKNOWLEDGMENTS

We would like to thank Diogo Almeida for his assistance and for allowing us to use the facilities in the Language, Mind and Brain Lab of New York University Abu Dhabi.

REFERENCES

[1] Omar AlZoubi, Rafael A. Calvo, and Ronald H. Stevens. 2009. Classification of EEG for affect recognition: An adaptive approach. In *Australasian Joint Conference on Artificial Intelligence*. Springer, 52–61.

[2] Bradley M. Appelhans and Linda J. Luecken. 2006. Heart rate variability as an index of regulated emotional responding. *Review of General Psychology* 10, 3, 229.

[3] Faisal Arafsha, Kazi Masudul Alam, and Abdulmotaleb El Saddik. 2015. Design and development of a user centric affective haptic jacket. *Multimedia Tools and Applications* 74, 9, 3035–3052.

[4] Jeremy N. Bailenson, Nick Yee, Scott Brave, Dan Merget, and David Koslow. 2007. Virtual interpersonal touch: Expressing and recognizing emotions through haptic devices. *Human–Computer Interaction* 22, 3, 325–353.

[5] Tonio Ball, Markus Kern, Isabella Mutschler, Ad Aertsen, and Andreas Schulze-Bonhage. 2009. Signal quality of simultaneously recorded invasive and non-invasive EEG. *Neuroimage* 46, 3, 708–716.

[6] Margaret M. Bradley and Peter J. Lang. 1994. Measuring emotion: The self-assessment manikin and the semantic differential. *Journal of Behavior Therapy and Experimental Psychiatry* 25, 1, 49–59.

[7] Lindsay Brown, Bernard Grundlehner, and Julien Penders. 2011. Towards wireless emotional valence detection from EEG. In *Engineering in Medicine and Biology Society (EMBC'11) Annual International Conference of the IEEE*. IEEE, 2188–2191.

[8] Ross Buck. 1994. The neuropsychology of communication: Spontaneous and symbolic aspects. *Journal of Pragmatics* 22, 3-4, 265–278.

[9] Jongeun Cha, Mohamad Eid, Ahmad Barghout, ASM Rahman, and Abdulmotaleb El Saddik. 2009. HugMe: Synchronous haptic teleconferencing. In *Proceedings of the 17th ACM International Conference on Multimedia*. ACM, 1135–1136.

[10] Monisha Chakraborty and Shreya Das. 2012. Determination of signal to noise ratio of electrocardiograms filtered by band pass and Savitzky-Golay filters. *Procedia Technology* 4, 830–833.

[11] Manfred Clynes. 1977. *Sentics: The Touch of Emotions*. Anchor Press, New York, NY.

[12] Ruo-Nan Duan, Jia-Yi Zhu, and Bao-Liang Lu. 2013. Differential entropy feature for EEG-based emotion classification. In *Neural Engineering (NER), 2013 6th International IEEE/EMBS Conference on*. IEEE, 81–84.

[13] Elia Gatti, Giandomenico Caruso, Monica Bordegoni, and Charles Spence. 2013. Can the feel of the haptic interaction modify a user's emotional state?. In *World Haptics Conference (WHC'13)*. IEEE, 247–252.
[14] Antal Haans and Wijnand I. Jsselsteijn. 2006. Mediated social touch: A review of current research and future directions. *Virtual Reality* 9, 2-3, 149–159.
[15] Ali Israr and Ivan Poupyrev. 2011. Control space of apparent haptic motion. In *World Haptics Conference (WHC'11)*. IEEE, 457–462.
[16] Tanimu Ahmed Jibril and Mardziah Hayati Abdullah. 2013. Relevance of emoticons in computer-mediated communication contexts: An overview. *Asian Social Science* 9, 4, 201.
[17] Min-Ki Kim, Miyoung Kim, Eunmi Oh, and Sung-Phil Kim. 2013. A review on the computational methods for emotional state estimation from the human EEG. *Computational and Mathematical Methods in Medicine*, vol. 2013, 13 pages. DOI : 10.1155/2013/573734.
[18] Franklin B. Krohn. 2004. A generational approach to using emoticons as nonverbal communication. *Journal of Technical Writing and Communication* 34, 4, 321–328.
[19] Peter J. Lang, Margaret M. Bradley, and Bruce N. Cuthbert. 2008. International affective picture system (IAPS): Affective ratings of pictures and instruction manual. *Technical Report A-8*. Gainesville, FL: University of Florida, USA.
[20] Paul Lemmens, Floris Crompvoets, Dirk Brokken, Jack Van Den Eerenbeemd, and Gert-Jan de Vries. 2009. A body-conforming tactile jacket to enrich movie viewing. In *3rd Joint EuroHaptics Conference and Symposium on Haptic Interfaces for Virtual Environment and Teleoperator Systems (World Haptics'09)*. IEEE, 7–12.
[21] Rodrigo Lentini, Beatrice Ionascu, Friederike A. Eyssel, Scandar Copti, and Mohamad Eid. 2016. Authoring tactile gestures: Case study for emotion stimulation. *World Academy of Science, Engineering and Technology, International Journal of Computer, Electrical, Automation, Control and Information Engineering* 10, 11, 1862–1867.
[22] Antonella Mazzoni and Nick Bryan-Kinns. 2015a. How does it feel like? An exploratory study of a prototype system to convey emotion through haptic wearable devices. In *7th International Conference on Intelligent Technologies for Interactive Entertainment (INTETAIN'15)*. IEEE, 64–68.
[23] Troy McDaniel, Shantanu Bala, Jacob Rosenthal, Ramin Tadayon, Arash Tadayon, and Sethuraman Panchanathan. 2014. Affective haptics for enhancing access to social interactions for individuals who are blind. In *International Conference on Universal Access in Human-Computer Interaction*. Springer, 419–429.
[24] Neurobehavioral Systems Inc. 2017. Presentation. Retrieved November 14, 2017 from https://www.neurobs.com/.
[25] Lauri Nummenmaa, Enrico Glerean, Riitta Hari, and Jari K. Hietanen. 2014. Bodily maps of emotions. *Proceedings of the National Academy of Sciences* 111, 2, 646–651.
[26] Panagiotis C. Petrantonakis and Leontios J. Hadjileontiadis. 2011. A novel emotion elicitation index using frontal brain asymmetry for enhanced EEG-based emotion recognition. *IEEE Transactions on Information Technology in Biomedicine* 15, 5, 737–746.
[27] Abu Saleh Md Mahfujur Rahman, S. K. Alamgir Hossain, and Abdulmotaleb El Saddik. 2010. Bridging the gap between virtual and real world by bringing an interpersonal haptic communication system in second life. In *IEEE International Symposium on Multimedia (ISM'10)*. IEEE, 228–235.
[28] Jukka Raisamo, Roope Raisamo, and Veikko Surakka. 2013. Comparison of saltation, amplitude modulation, and a hybrid method of vibrotactile stimulation. *IEEE Transactions on Haptics* 6, 4, 517–521.
[29] Debra L. Roter, Richard M. Frankel, Judith A. Hall, and David Sluyter. 2006. The expression of emotion through nonverbal behavior in medical visits. *Journal of General Internal Medicine* 21, S1, S28–S34.
[30] Katri Salminen, Veikko Surakka, Jani Lylykangas, Jukka Raisamo, Rami Saarinen, Roope Raisamo, Jussi Rantala, and Grigori Evreinov. 2008. Emotional and behavioral responses to haptic stimulation. In *Proceedings of the SIGCHI Conference on Human Factors in Computing Systems*. ACM, 1555–1562.
[31] Louis A. Schmidt and Laurel J. Trainor. 2001. Frontal brain electrical activity (EEG) distinguishes valence and intensity of musical emotions. *Cognition & Emotion* 15, 4, 487–500.
[32] Mohammad Soleymani, Maja Pantic, and Thierry Pun. 2012. Multimodal emotion recognition in response to videos. *IEEE Transactions on Affective Computing* 3, 2, 211–223.
[33] Kai Sun, Junqing Yu, Yue Huang, and Xiaoqiang Hu. 2009. An improved valence-arousal emotion space for video affective content representation and recognition. In *IEEE International Conference on Multimedia and Expo (ICME'09)*. IEEE, 566–569.
[34] Dzmitry Tsetserukou, Alena Neviarouskaya, Helmut Prendinger, Mitsuru Ishizuka, and Susumu Tachi. 2010. iFeel_IM: Innovative real-time communication system with rich emotional and haptic channels. In *CHI'10 Extended Abstracts on Human Factors in Computing Systems*. ACM, 3031–3036.
[35] Xiao-Wei Wang, Dan Nie, and Bao-Liang Lu. 2014. Emotional state classification from EEG data using machine learning approach. *Neurocomputing* 129, 94–106.
[36] Joyce H. D. M. Westerink, Egon L. Van Den Broek, Marleen H. Schut, Jan Van Herk, and Kees Tuinenbreijer. 2008. Computing emotion awareness through galvanic skin response and facial electromyography. In *Probing Experience*. Springer, 149–162.

[37] Yongjae Yoo, Taekbeom Yoo, Jihyun Kong, and Seungmoon Choi. 2015. Emotional responses of tactile icons: Effects of amplitude, frequency, duration, and envelope. In *IEEE World Haptics Conference (WHC'15)*. IEEE, 235–240.
[38] Xu Zhe and A. C. Boucouvalas. 2002. Text-to-emotion engine for real time Internet communication. In *Proceedings of International Symposium on Communication Systems, Networks and DSPs*. 164–168.
[39] Wei-Long Zheng, Jia-Yi Zhu, and Bao-Liang Lu. 2016. Identifying stable patterns over time for emotion recognition from EEG. *Arxiv Preprint Arxiv:1601.02197*.

Received March 2017; revised June 2017; accepted August 2017